

Characterization of Probe Binding and Comparison of Its Influence on Fluorescence Lifetime of Two pH-Sensitive Benzo[c]xanthene Dyes Using Intensity-Modulated Multiple-Wavelength Scanning Technique

Ronnie M. Andersson,^{*,1} Kjell Carlsson,[†] Anders Liljeborg,^{†,‡} and Hjalmar Brismar^{*}

^{*}Department of Woman and Child Health, Karolinska Institutet, Astrid Lindgren Children's Hospital, SE-171 76 Stockholm, Sweden; and [†]Department of Biomedical and X-Ray Physics, and [‡]Department of Physics of Nanostructures, Royal Institute of Technology, SE-100 44 Stockholm, Sweden

Received February 10, 2000

Quantitative pH imaging using the carboxy seminaphthofluorescein dyes SNAFL-1 and SNAFL-2 can be performed by measurement of intensity ratios or fluorescence lifetimes. However, there is a controversy as to whether the latter method has the practical advantage of a straightforward pH calibration in buffers compared to a cumbersome and time-consuming procedure in cells. In this study we have undertaken a systematic study of the potential factors influencing the fluorescence lifetime of the probes at different pH using confocal microscopy. *In vitro* results demonstrate that factors such as lipid and protein concentrations have a substantial influence on pH measurements based on fluorescence lifetime. The pH could be overestimated by more than 2 pH units. Studies in permeabilized COS-7 cells demonstrate the same trends as observed in the *in vitro* studies. © 2000 Academic Press

Press

Key Words: confocal microscopy; fluorescence lifetime imaging; pH measurement; COS-7; SNAFL-1; SNAFL-2.

Cellular processes, such as growth and proliferation, are often accompanied by changes in intracellular H⁺ concentration. A variety of fluorescent pH indicators are available for biological use (1, 2). A particularly interesting class of pH probes are the long-wavelength benzo[c]xanthene dyes consisting of seminaphthofluo-

resceins (SNAFLs)² and seminaphthorhodafluors (SNARFs) (3). These pH probes exhibit a number of desirable properties such as distinct emission from the protonated and deprotonated forms, absorption maxima near the visible lines of the argon laser, and long-wavelength emission. The carboxylated forms of these dyes are well retained inside the cell, due to a pK_a value that is near to that observed in living cells.

Quantitative pH measurement in cells using SNAFL and SNARF can be performed using either ratios of intensity measurements or fluorescence lifetimes (3–6). With these probes, the emission intensity at one of the wavelengths is pH independent, while at another wavelength it is pH dependent. Hence, estimation of pH from the ratio of emission intensities at the two wavelengths will correct for shortcomings such as photobleaching and leakage of dye. However, the ratiometric procedure cannot correct for probe binding (5). Binding of probes to macromolecules and membranes could result in significant changes in emission spectrum and quantum yield with apparent shift in the acid-base equilibrium of the probe. Extracellular calibration using the ratiometric method is therefore not possible.

Lifetime-based pH measurements are based on the fluorescence lifetime differences for the protonated and deprotonated forms of the probe. The fluorescence lifetime is generally independent of probe concentration and thus insensitive to photobleaching and leakage. A

¹ To whom correspondence should be addressed at Research Laboratory Q2:09, Astrid Lindgren Children's Hospital, SE-171 76 Stockholm, Sweden. Fax: +46-(0)8-51777328. E-mail: Ronnie.Andersson@kbh.ki.se. Homepage: www.ki.se/kbh/pediatrik.

² Abbreviations used: SNAFLs, seminaphthofluoresceins; SNARFs, seminaphthorhodafluors; IMS, intensity-modulated multiple-wavelength scanning; PSS, physiological buffer solution; BSA, bovine serum albumin; PMT, photomultiplier tube.

suggested practical advantage of lifetime imaging is the straightforward calibration in buffers rather than the cumbersome and time-consuming procedures in cells. However, there is a controversy as to whether extracellular calibration is possible or not using fluorescence-lifetime-based pH measurements.

Recently two reports described fluorescence lifetime measurement of two similar pH probes: cSNAFL-1 and cSNARF-1 (4, 5). Sanders *et al.* (4) found that cSNAFL-1 exhibits a weak dependence on variables such as hydrophobicity and cellular composition. However, Srivastava and Krishnamoorthy (5) showed that cSNARF-1 lifetime is influenced by macromolecules and that such probe binding could overestimate the intracellular pH by as much as 1 pH unit. They also suggested a correction for probe binding. However, their method measures average cytoplasmic pH, and therefore does not take into account pH differences and their spatial locations inside the cell.

In this study we have undertaken a systematic study of the potential factors influencing the fluorescence lifetime of the probes cSNAFL-1 and cSNAFL-2 at different pH using the intensity-modulated multiple-wavelength scanning (IMS) technique (7). Although the structural difference between the two dyes is only an extra chloro atom in cSNAFL-2, they have different binding properties.

MATERIALS AND METHODS

Cell Culture

COS-7 cells, a monkey kidney cell line, were grown at 37°C, in 5% CO₂ and 95% humidified air, on 100-mm culture dishes in complete DMEM, supplemented with 10% fetal calf serum and 1% penicillin/streptomycin (8). Medium was changed every 4 days until the cells were confluent and subsequently replated. On the day before the experiment, cells were replated on glass coverslips (Ø60 mm) at a density of 5×10^5 cells per coverslip.

Buffer Preparation

Probes (carboxy SNAFL-1: 5'-(and 6')-carboxy-3,10-dihydroxy-spiro[7*H*-benzo[*c*]xanthene-7,1'-(3'-*H*)-isobenzofuran]-3'-one; and carboxy SNAFL-2: 5'-(and 6')-carboxy-9-chloro-3,10-dihydroxyspiro[7*H*-benzo[*c*]xanthene-7,1'-(3'-*H*)-isobenzofuran]-3'-one) were obtained from Molecular Probes Europe BV. The final concentration of probes was 30 μM prepared from a 1 mM stock solution in DMSO. The pH in the range 6.0 to 9.0 was achieved by adding NaOH or HCl to a physiological buffer solution (PSS) containing (in mM) 100 NaCl, 4.0 KCl, 0.1 CaCl₂, 1.2 MgCl₂, 1 Na₂HPO₄, 25 NaHCO₃, 20 *N*-2-hydroxyethylpiperazine-*N'*-2-ethanesulfonic acid (Hepes), 10 glucose, pH 7.4 adjusted

with Trizma base. To the PSS we added 0.1% (v/w) saponin. Protein solutions in the range from 0 to 100 mg/ml were prepared by dissolving bovine serum albumin (BSA) (Sigma, St. Louis, MO) powder in PSS.

A crude extract from sheep brain (L-α-phosphatidylethanolamine) (Sigma) containing several phospholipids and glycolipids normally found in brain tissue was used for lipid solutions. Three concentrations of lipid solution were used: low (1 mg/ml), medium (10 mg/ml), and high (saturated solution). The lipid solutions were sonicated for 2 min.

To compare cell conditions with *in vitro* studies, we mimicked the cell situation with mixtures of protein and lipid. Mixtures of protein and lipid solutions were prepared by mixing equal volumes of protein solution (100 mg/ml) and lipid solution (saturated solution). Protein solution containing 50 mg/ml and half-saturated lipid solution were prepared as controls.

All protein and lipid solutions were adjusted to pH 6.0 and 9.0 following preparation and were recorded in 0.20-mm glass capillaries. Extracellular calibration curves of the probes in PSS were recorded from pH 6.0 to 9.0 in 0.20-mm glass capillaries. All capillaries were mounted on an objective glass and sealed with Entellan (Merck, Darmstadt, Germany).

Cell Preparation

COS-7 cells were examined at pH 6.0 and 9.0. Cells were washed three times with PSS buffer containing 0.1% saponin at pH 6.0 and 0.005% at pH 9.0 and then incubated in 30 μM of probe (cSNAFL-1/cSNAFL-2) in the same buffer respectively for 30 min at room temperature. Saponin was used to enable loading of the cell with the cell impermeable probe. Saponin treatment was more efficient at pH 9.0 than at pH 6.0; hence, the lower concentration was used. Cell pH was then recorded with the cells still in the incubation buffer, where the background fluorescence served as control.

Image Recording Technique

The pH was measured with the IMS technique (9–12). In this technique, the specimen is illuminated with intensity-modulated laser light (frequency, $f = 23$ MHz, wavelength, $\lambda = 488$ nm), and the specimen is imaged through a confocal microscope (Fig. 1). Fluorescent light with a wavelength longer than 515 nm was detected by a photomultiplier tube (PMT). The fluorescent light will have the same modulation frequency as the modulating light, but will be phase shifted in relation to the fluorescence lifetime of the probe. This relation is described by (13)

$$\alpha = \text{atan}(\omega\tau),$$

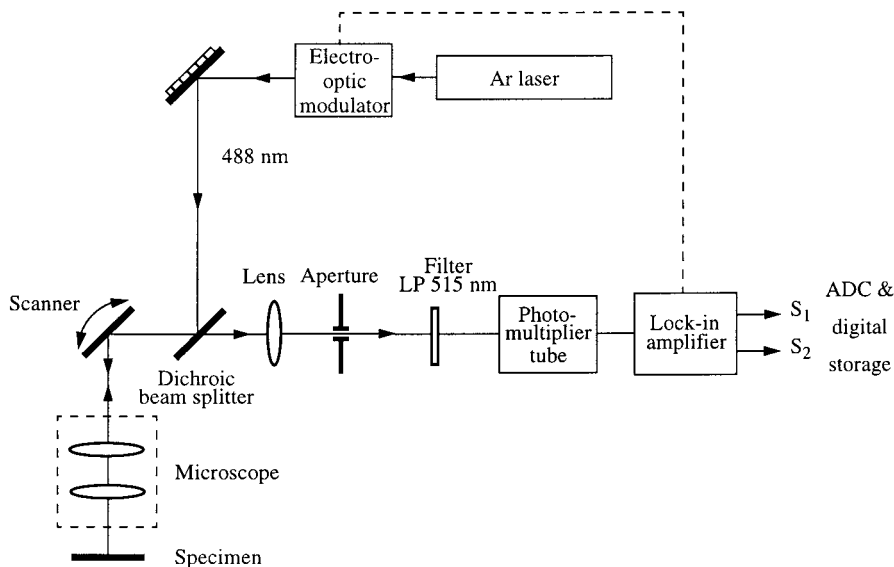


FIG. 1. The experimental setup for measuring pH with confocal fluorescence lifetime imaging using a pH-sensitive probe. The argon ion laser which illuminates the specimen is modulated by an electro-optic modulator (EOM). The excitation light enters the confocal microscope via the phototube. The fluorescent light passes through a dichroic beam splitter and the confocal aperture and reaches the photomultiplier tube (PMT) detector via a long pass filter. The detector output signal enters the lock-in amplifier which is phase-locked to the modulating frequency. Here frequency- and phase-selective detection produces two output signals S_1 and S_2 . The ratio S_1/S_2 is calibrated using a reference specimen of known pH. In this way the ratio can be translated into pH.

where α is the phase angle, $\omega = 2\pi f$, and τ is the fluorescence lifetime of the probe. The signal from the PMT is passed through a frequency- and phase-selective amplifier (lock-in amplifier) "tuned" to the modulation frequency. The "in-phase" and "quadrature" output signals from the lock-in amplifier (S_1 and S_2 in Fig. 1) are digitized and stored in the computer as digital images of the specimen. From these output signals the phase angle α , and thereby the lifetime τ , can be calculated (11, 12). However, the ratio of the output signals, S_1 and S_2 , can be directly correlated to pH units via calibration data from glass capillaries. It is therefore not necessary to calculate lifetime values. Using this technique, we created images where pixel values correspond to pH (14). The sensitivity is such that a pH difference of 0.1 units can easily be detected in an 8-bit digital image (7). Background images were also recorded (laser excitation light blocked) and subtracted to correct for offsets in the recordings. A threshold was applied prior to computing the ratio, thereby rendering the background black (zero).

RESULTS AND DISCUSSION

Effect of Proteins

The effect of the presence of proteins on the lifetime-based pH measurements was investigated by imaging cSNAFL-1 or cSNAFL-2 in buffers containing different concentrations of BSA (Fig. 2).

cSNAFL-1: At pH 6.0, different protein concentrations had no effect on lifetime-based pH. At pH 9.0, the

presence of protein caused a concentration-dependent decrease of lifetime-based pH. At the maximum protein concentration used, pH was underestimated by 1.2 units.

cSNAFL-2: At pH 6.0, the presence of protein caused a concentration-dependent increase in lifetime-based pH. An increase in protein concentration from 1 to 10 mg/ml caused an overestimate in pH from 0.5 to 2.1 units. At pH 9.0, the protein effect was small but pH was underestimated with increasing protein concentration.

The opposite effect of protein concentration on lifetime-based pH seen with both cSNAFL-1 and cSNAFL-2 at pH 6.0 and 9.0 indicates that even small structural differences may have major effects on probe binding to proteins and that this is dependent not only on protein concentration but also on pH.

Even though BSA was used here, the pH dependence of probe binding indicates that the effect of protein concentration on fluorescence lifetime will vary with the isoelectric point of the protein involved.

Effect of Lipids

A crude extract from sheep brain (L- α -phosphatidylethanolamine) containing several phospholipids and glycolipids normally found in brain tissue was used in lipid solutions together with cSNAFL-1 or cSNAFL-2 (Fig. 3). Three concentrations of lipid solution were used: low (1 mg/ml), medium (10 mg/ml), and high (saturated solution).

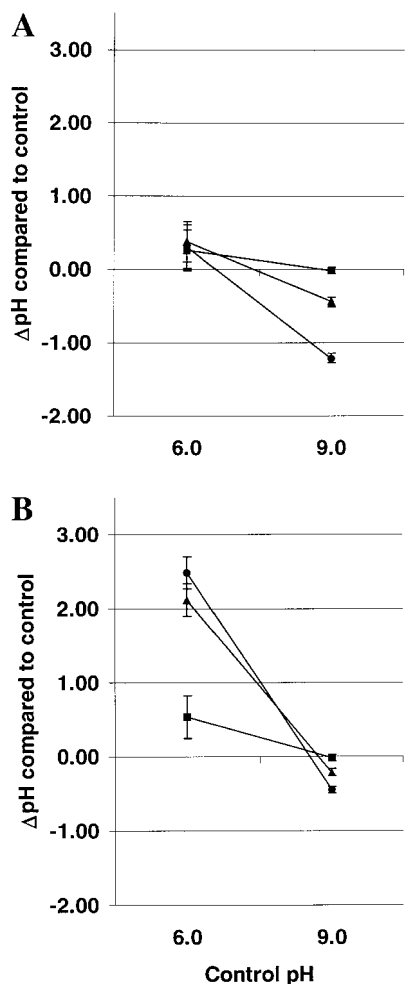


FIG. 2. The effect of proteins on the lifetime-based pH of cSNAFL-1 (A) and cSNAFL-2 (B) was investigated in glass capillaries with different concentrations of BSA (■, 1 mg/ml; ▲, 10 mg/ml; and ●, 100 mg/ml; $n = 5$).

cSNAFL-1: At pH 6.0, low and medium concentrations of lipid had minor effects on the lifetime-based pH. However, at high lipid concentration the measured pH was significantly increased and a pH overestimate of 2.2 units was observed. At pH 9.0, a small but concentration-dependent increase in pH was also seen. High lipid concentration had a four times greater effect on lifetime-based pH than medium lipid concentration (+0.4 vs +0.1).

cSNAFL-2: The effect at pH 6.0 was similar to that observed for cSNAFL-1 at the same pH. In contrast at pH 9.0, lipid solutions produced an underestimate of lifetime-based pH compared to cSNAFL-1.

The effect of lipids was greater at pH 6.0 than at pH 9.0, especially at the highest lipid concentration. It is known that probe binding by lipids is less pH sensitive and more concentration dependent. These results were expected since lipids have very few polar groups which

are pH sensitive, i.e., amino, carboxy, and phosphate groups, compared to proteins. Lipids are probably interacting in the same fashion with both fluorophores regardless of their slight structural difference.

Combined Effect of Lipids and Proteins

The behavior of the lifetime-based pH of cSNAFL-1 and cSNAFL-2 in solutions containing both lipids and proteins was studied at pH 6.0 and 9.0 (Fig. 4).

cSNAFL-1: At pH 6.0, lipid + protein produced an overestimate in lifetime-based pH, although lipid had the most profound effect. There was no difference in measured pH between lipid + protein and protein at pH 9.0; thus, at this pH, protein can account for the entire effect of lipid + protein on lifetime-based pH.

cSNAFL-2: At pH 6.0, lipid + protein produced a large overestimate in lifetime-base pH, with the lipid

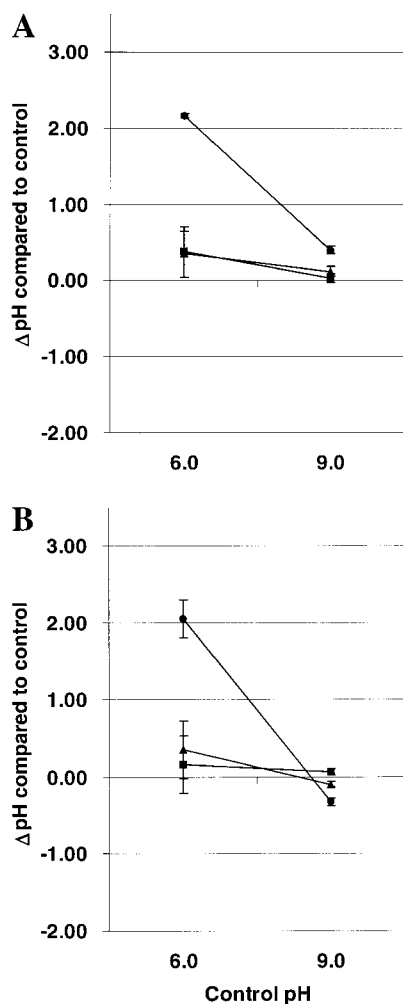


FIG. 3. The effect of lipids on the lifetime-based pH of cSNAFL-1 (A) and cSNAFL-2 (B) was investigated in glass capillaries with different concentrations of lipids (■, low, 1 mg/ml; ▲, medium, 10 mg/ml; and ●, high saturated; $n = 5$).

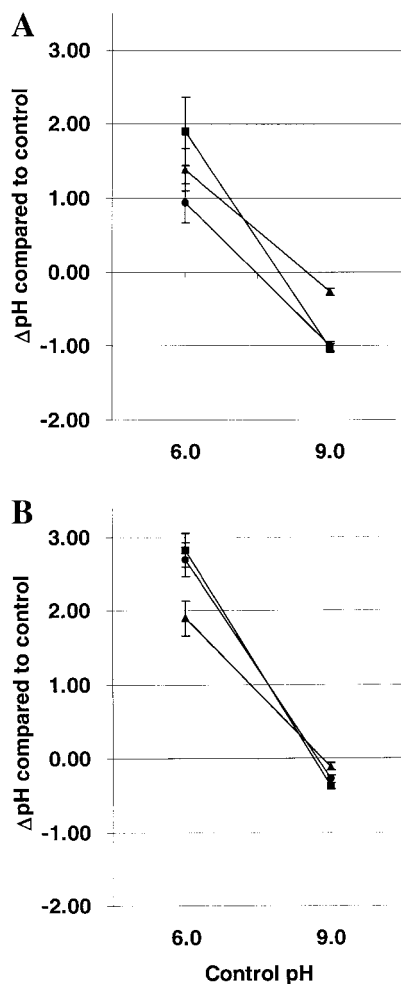


FIG. 4. The combined effect of lipids and proteins on the lifetime-based pH of cSNAFL-1 (A) and cSNAFL-2 (B) was investigated in capillaries with 50 mg/ml of BSA in half-saturated lipid solution (■, lipid half-saturated + protein 50 mg/ml; ▲, lipid half-saturated; and ●, protein 50 mg/ml; $n = 5$).

contribution to this effect being less than that of protein. At pH 9.0, lipid + protein produced a minor but additive underestimate of monitored pH.

Lipid exerts an effect on measured pH but is less pronounced than that of protein. Only where the two probes were less affected by protein, pH 6.0 for cSNAFL-1 and pH 9.0 for cSNAFL-2, was the influence of lipid larger than that of protein.

Effect in Cells

Intracellular calibration was first carried out in cells loaded with cell-membrane-permeable probe, cSNAFL-2 AM ester, and made selectively permeable for H^+ ions by adding the drug nigericin and KCl with a final concentration of 150 mM KCl to the cell buffer (15–17). This ensures equilibration of the pH between

cells and medium. However, only a small effect on measured intracellular pH was observed using this calibration protocol at both pH 6.0 and 9.0 (15). We therefore developed a protocol for intracellular calibration with a built-in control. COS-7 cells were incubated for 30 min in buffer containing cell-impermeable cSNAFL-1 or cSNAFL-2 with 0.1% saponin at pH 6.0 or 0.005% saponin at pH 9.0 (Fig. 5). Intracellular pH imaging was then performed without change of medium and the background fluorescence served as pH control. Without saponin the cell-impermeable probes did not enter the cells, which appeared as dark objects with a bright surrounding halo (data not shown). This method proved to be useful, but we suspected leakage of cell contents into the extracellular buffer and thereby reducing the magnitude of overall effect of probe binding on the measured lifetime-based pH.

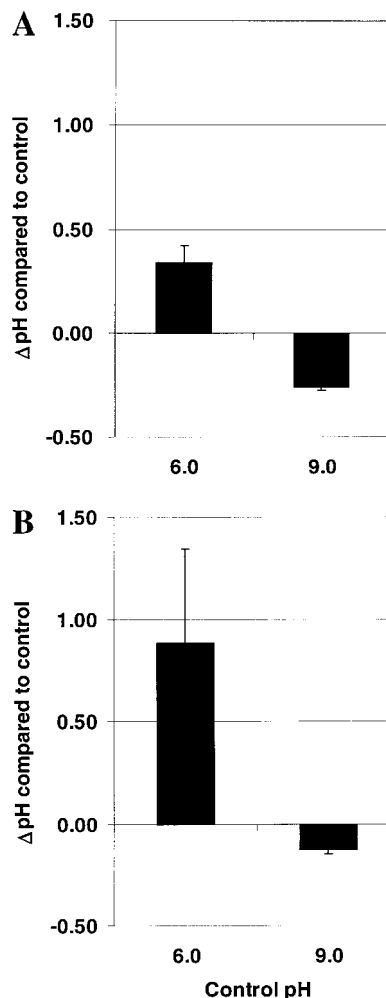


FIG. 5. The effect on the lifetime-based pH of cSNAFL-1 (A) and cSNAFL-2 (B) was investigated in permeabilized COS-7 cells (20 observations, cell measurements, in all of 3 coverslips).

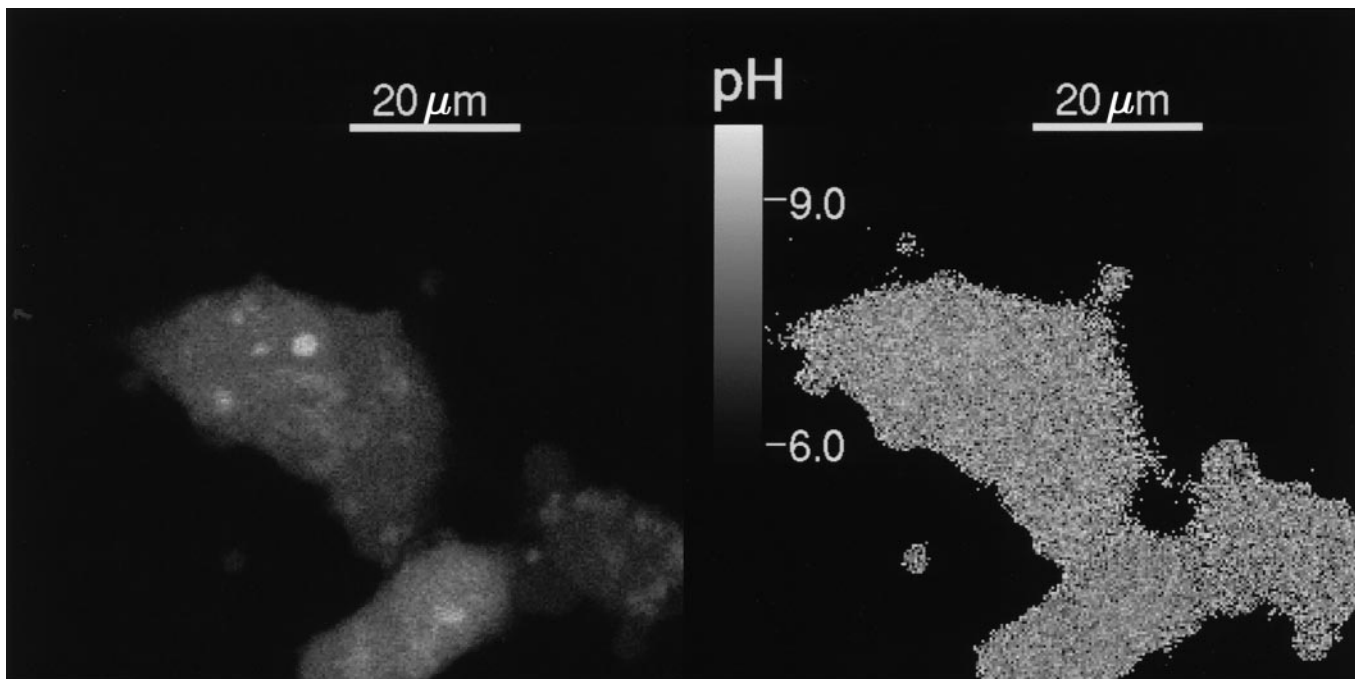


FIG. 6. Confocal intensity and lifetime image of COS-7 cell loaded with cSNAFL-2 AM ester ($30 \mu\text{M}$). Intracellular pH in living cells was 7.8 ± 0.10 pH units ($n = 6$). Strangely, intracellular pH is constant throughout the whole cell.

cSNAFL-1: At pH 6.0, cell contents caused an overestimate of 0.3 pH units on lifetime-based pH. At pH 9.0, there was an underestimate of 0.3 pH units.

cSNAFL-2: The effect at pH 6.0 was more pronounced with an overestimate of 0.9 pH units on measured pH. At pH 9.0, there was a small underestimate of 0.1 pH units.

The observed effects in cells agrees well with the combined effect of protein and lipid: i.e., an overestimate of lifetime-based pH at pH 6.0 and an underestimate of lifetime-based pH at 9.0. The effect in cells was less pronounced, likely due to leakage of cell contents.

Quantitative pH Imaging in Cells

Intracellular pH imaging in COS-7 cells was performed using cSNAFL-2 AM ester and extracellular calibration. Intracellular pH in living cells was 7.8 ± 0.10 pH units ($n = 6$) compared to the normal intracellular cytoplasmic pH of approximately 7.2 pH units. We expected to find spatial pH differences within the cells due to organelles, i.e., mitochondria, and other structures, i.e., lysosomes. However, these domains were not identifiable in the pH lifetime image (Fig. 6). These findings are in agreement with a previous study with cSNAFL-1 utilizing both emission ratio and lifetime imaging in cells (4). The measured uniform pH throughout the whole cell indicates a serious limitation of the fluorescent pH imaging method.

This study indicates that fluorescence lifetime is substantially influenced by protein and lipid concentrations. It is a well known fact that the cell is a crowded environment of proteins: Muscle cells contain approximately 23% protein by weight; red blood cells contain about 35% protein by weight; and, in general, actively growing cells contain between 17 and 26% protein by weight (18). Thus, there are reasons to believe that the fluorescence lifetime is influenced by varying cytoplasmic concentrations of lipids and proteins. This in turn may mask the pH differences inside the cell. Interestingly, probe binding correction has been suggested by Srivastava *et al.* (5). However, this is not directly applicable to the IMS technique, but it is, in principle, possible to strongly reduce errors by making multiple measurements at different modulation frequencies.

CONCLUSION

Our study on the influence of probe binding on pH based on fluorescence lifetime indicates that the method is not a straightforward approach to measure pH in the absence of correction for the effect of probe binding. This is in agreement with a previous study using time-resolved fluorescence microscopy (5). We find it likely that other fluorescent ion probes have a probe-binding-sensitive fluorescence lifetime. However, this effect is hard to predict. Here, we show that the effect of probe binding is different even with small

structural differences between fluorophores, as such as between cSNAFL-1 and cSNAFL-2.

Apart from H⁺ ions, protein concentration has a major effect on the fluorescence lifetime for both cSNAFL-1 and cSNAFL-2. In general, lipids exerted less influence on fluorescence lifetime, independent of pH, compared to that of proteins. The similar results from the combined effects of lipids and proteins and the effects in cells on cSNAFL-1 and cSNAFL-2 indicate that the protein- and lipid-dense cytoplasm of cells alters the lifetime-based estimate of pH, producing a homogenous intracellular pH throughout the cell interior.

ACKNOWLEDGMENTS

The authors thank Professor Gerald F. DiBona (University of Iowa) and Professor Gunnar von Heijne (Stockholm University) for many useful suggestions and comments. This work was financially supported by the Swedish Medical Research Council, the Swedish Research Council for Engineering Sciences, Anders Wall Foundations, and Carl Trygger Foundation.

REFERENCES

1. Vicentini, L. M., and Villereal, M. L. (1986) *Life Sci.* **38**, 2269–2276.
2. Kubohara, Y., and Okamoto, K. (1991) *FASEB J.* **8**, 869–874.
3. Whitaker, J. E., Haugland, R. P., and Prendergast, F. G. (1991) *Anal. Biochem.* **194**, 330–344.
4. Sanders, R., Draaijer, A., Gerritsen, H. C., Houpt, P. M., and Levine, Y. K. (1995) *Anal. Biochem.* **227**, 302–308.
5. Srivastava, A., and Krishnamoorthy, G. (1997) *Anal. Chem.* **249**, 140–146.
6. Krishnamoorthy, G., and Srivastava, A. (1997) *Curr. Sci.* **72**, 835–845.
7. Carlsson, K., Liljeborg, A., Andersson, R. M., and Brismar, H. (2000) *Proc. SPIE Vol. 3919*, pp. 30–37, San José, CA.
8. Andersson, R. M., Cheng, S. X. J., and Aperia, A. (1998) *Acta Physiol. Scand.* **164**(1), 39–46.
9. Åslund, N., and Carlsson, K. (1993) *Micron* **24**, 603–609.
10. Carlsson, K. (1995) *Micron* **26**, 317–322.
11. Carlsson, K., and Liljeborg, A. (1997) *J. Microsc.* **185**, 37–46.
12. Carlsson, K., and Liljeborg, A. (1998) *J. Microsc.* **191**, 119–127.
13. Spencer, R. D., and Weber, G. (1969) *Ann. NY Acad. Sci.* **158**, 361–376.
14. Liljeborg, A., Carlsson, K., and Andersson, R. M. (1998) *Proc. SPIE, Vol. 3568*, pp. 82–88, Stockholm, Sweden.
15. Andersson, R. M., Carlsson, K., Liljeborg, A., and Brismar, H. (2000) *Proc. SPIE Vol. 3921*, pp. 242–248, San José, CA.
16. Thomas, J. A., Buchsbaum, R. N., Zimniak, A., and Racker, E. (1979) *Biochemistry* **18**, 2210–2218.
17. Rink, T. J., Tsien, R. Y., and Pozzan, T. (1982) *J. Cell Biol.* **95**(1), 189–196.
18. Siekevitz, L. A. (1969) *Cell Structure and Function*, Holt, Rinehart & Winston, New York.